Published in final edited form as:

*J Immunol*. 2018 April 15; 200(8): 2748–2756. doi:10.4049/jimmunol.1701492.

# Intracellular nucleic acid sensing triggers necroptosis through synergistic type-I interferon and TNF signaling

**Michelle Brault**[1,2], **Tayla M. Olsen**[1], **Jennifer Martinez**[3], **Daniel B. Stetson**[1,*], and **Andrew Oberst**[1,*]

[1]Department of Immunology, University of Washington, 750 Republican St. Seattle, WA USA 98109

[2]Molecular and Cellular Biology Program, University of Washington, 1959 NE Pacific St, HSB T-466 Seattle, WA USA 98195

[3]Immunity, Inflammation, and Disease Laboratory, NIEHS, National Institutes of Health, 111 T W Alexander Dr. Research Triangle Park, Durham, NC USA 27709

## Abstract

The sensing of viral nucleic acids within the cytosol is essential for the induction of innate immune responses following infection. However, this sensing occurs within cells that have already been infected. The death of infected cells can be beneficial to the host by eliminating the virus's replicative niche and facilitating the release of inflammatory mediators. Here, we show that sensing of intracellular DNA or RNA by cGAS-STING or RIG-I-MAVS, respectively, leads to activation of RIPK3 and necroptosis in bone marrow-derived macrophages. Notably, this requires signaling through both type I interferon (IFN) and tumor necrosis factor (TNF) receptors, revealing synergy between these pathways to induce cell death. Furthermore, we show that hyper-activation of STING in mice leads to a shock-like phenotype, the mortality of which requires activation of the necroptotic pathway and IFN and TNF co-signaling, demonstrating that necroptosis is one outcome of STING signaling *in vivo*.

### Keywords

Innate immunity; cell death; antiviral response

## Introduction

The induction of programmed cell death is an important process for maintaining tissue homeostasis, as well as improving immune system function. While billions of cells in our bodies die each day by apoptosis, the induction of lytic cell death programs during infection more readily instruct and aid our immune system. One such cell death program is programmed necrosis, or necroptosis, which is both morphologically and mechanistically

*Correspondence to: stetson@uw.edu, oberst@uw.edu.

**Disclosures**

The authors declare no competing interests.

distinct from apoptosis, and requires the activation of receptor interacting protein kinases 1 and 3 (RIPK1 and RIPK3)(1). Notably, RIPK3-deficient animals display increased susceptibility to a variety of viral infections(2–6) highlighting the role of this pathway in antiviral host defense. Furthermore, cells deficient in type-I interferon (hereafter IFN) signaling, an essential component of antiviral defense, fail to induce necroptosis following treatment with a variety of RIPK3-activating stimuli(7), suggesting that necroptosis may constitute an arm of the IFN-driven antiviral response.

The sensing of foreign nucleic acids is a key initiating event in the innate immune response to viral infection. The presence of DNA in the cytosol is one such signature of infection. In most cell types, cytosolic DNA activates the cGAS-STING pathway(8). Briefly, cGAS senses DNA and synthesizes the secondary messenger cyclic GMP-AMP (cGAMP)(9), which binds directly to STING(10), leading to activation of TBK-1 and IRF3-dependent transcription of IFNβ(11). The production and signaling of type I IFN leads to the induction of hundreds of IFN-stimulated genes (ISGs), inducing an antiviral state. As such, cGAS or STING-deficient mice are highly susceptible to infection by various DNA viruses(12–15). Intriguingly, many of these viruses also lead to significant mortality in RIPK3-deficient animals(2, 3, 5, 16). A recent study found that murine gammaherpesvirus-68 (MHV68) could induce necroptosis in L929 cells, and that this response was prevented by knockdown of STING(17). However, given the complex cellular responses triggered by viral infection, coupled with the observation that L929 cells constitutively express and respond to TNF in an autocrine manner(18), the mechanistic and physiological links between STING signaling and necroptosis remain unclear.

Here we show that the sensing of cytosolic DNA induces programmed necrosis through the activation of the cGAS-STING pathway in primary cells. Interestingly, robust activation of cell death by this pathway requires not only type I IFN signaling, but also an intact TNF signaling pathway. Furthermore, we show that RNA ligands acting through the sensors TLR3 or RIG-I also require both IFN and TNF signaling to induce necroptosis, highlighting the essential synergy between these signaling pathways in response to a variety of innate immune stimuli. Finally, we find that *in vivo* administration of a STING agonist leads to a fatal, shock-like inflammatory disease in mice. Mortality associated with this disease requires both TNF and IFN signaling, and is significantly rescued in animals lacking components of the necroptotic pathway. These results indicate that multiple nucleotide sensing pathways can trigger necroptosis through the synergistic action of the IFN and TNF, and that this signaling can mediate lethal shock in mice.

## Materials and Methods

### Cell culture, transfection protocol, and reagents

Macrophages were differentiated for seven days from whole bone marrow in RMPI (HyClone) with 10% CMG12–14 supernatant, 10% FBS (Gemini), 100 units/ml penicillin/streptomycin (HyClone), 2mM glutamine (HyClone), 50 mM beta-mercaptoethanol, and 10 mM HEPES (HyClone). Macrophages were lifted with 4mM EDTA in PBS, counted, and plated at 150,000 cells/well in 24 well plates for death assays. Primary MEFs were cultured in DMEM (HyClone) with 10% FBS (Gemini), 100 units/ml penicillin/streptomycin

(Hyclone), 2mM glutamine (HyClone), 10 mM HEPES (HyClone), and 1 mM sodium pyruvate (HyClone). Cell death assays were done using the IncuCyte bioimaging platform (Essen); four images per well were captured, analyzed, and averaged. Death was measured by the incorporation of Sytox green (Life Tech) and normalized to starting total cell count using Syto green (Life Tech). zVAD-FMK (SM Biologicals) was used at a concentration between 25–50 μM depending on application. Experiments where zVAD treatment alone exceeded 40% cell death were eliminated from analysis as background was deemed too high for reliable death data, though these experiments never showed trends not consistent with data shown. Transfections were done at a 1:1 ratio with Lipofectamine 2000 (Life Tech) and 2 μg/ml of calf thymus DNA (Sigma) or 2′3′-cGAMP (Invivogen), unless otherwise specified. ISD (interferon stimulatory DNA) was annealed as previously described(11) and transfected at a concentration of 2 μg/ml. Poly(I:C) (EMD Millipore) was added directly to the media at 1 μg/ml. RIG-I ligand (5′ triphosphate RNA) was transcribed and purified as previously described(19) using a T7 Megashortscript kit (Ambion) and then transfected at a concentration of 1μg/ml. High dose IFN A (PBL Assay Science) for cell death assay was 100 units/ml, based on the specific activity of each lot. For Luminex panels, macrophages were transfected with each ligand and supernatants were collected after 6 hours and frozen at −80 until analyzed per manufacturer's guidelines.

## Mice

All animals used in this study, either as a source of primary cells or for *in vivo* analysis, have been previously described. These include animals lacking cGAS(20), STING(21), IFNAR1 (provided by M.K. Kaja and described in (22)), TNF (Jax stock #003008), TNFR1 (Jax stock #002818), TNFR2 (Jax stock #002620), DAI(generated in (23) and kindly provided by Dr. William Kaiser), AIM2 (Jax stock #013144), Caspase1 and 11 (Generated in (24) and kindly provided by Dr. Michael Gale), RIPK3(25), MLKL(26), MAVS (kindly provided by Drs. M. Loo and M. Gale, U. of Washington), TLR3(27), STAT1 (kindly provided by Dr. Herbert W. Virgin) and STAT2 (Jax stock #023309). All animals used were backcrossed to the C57BL/6J background, with the exception of RIPK3 knockouts as described.

## DMXAA injection

Animals use for *in vivo* analysis, including wild-type controls, were bred and housed in the UW animal facility. Animals were injected intraperitoneally with 40mg/kg DMXAA (MedKoo) resuspended in 84% PBS, 10% $NaHCO_3$ (5% in $H_2O$), and 6% DMSO. Weights, surface temperatures, and clinical signs were monitored at 0, 4, 6, 8, 12, and 24 hours post injection. Clinical score was determined by appearance and clinical signs; scores were additive for each sign and animals with cumulative scores of nine or above were euthanized. Sign (score): Lack of grooming (1), ocular discharge (2), hunched (2), duck walk (4), weight loss between 15–20% of starting body weight (4), lethargic (6), weakly responsive or surface temperature less than 28.5° C (8), weight loss greater than 20% of starting body weight, moribund, or surface temperature less than 27.5° C (9). To determine serum cytokines, blood was collected 6 hours post injection by terminal heart puncture. Mice for serum collection were selected randomly prior to injection and were not included in survival data. TNF and IL-6 in serum was measured using ELISA (eBioscience) according to manufacturer's direction.

### Western blots

Macrophages were lysed in buffer containing 20mM Tris HCl (pH 7.5), 135mM NaCl, 1.5mM $MgCl_2$, 1mM EGTA, 1% Triton X-100, 10% glycerol, and 2X Pierce protease/phosphatase inhibitor mini tablets (Fisher). Thirty micrograms of protein were run on 4%–12% Novex Tris-Glycine gel (Fisher) in running buffer (24mM Tris, 32mM glycine, 3.5mM SDS) and transferred to a PVDF membrane (Thermo) in transfer buffer (6mM Tris, 8mM glycine, 20% methanol). Membranes were blocked overnight in 5% bovine serum albumin (BSA) in TBS plus 1% Tween20 (TBST). Membranes were incubated overnight with primary antibody in 5% BSA in TBST. Membranes were incubated with HRP-conjugated secondary antibodies for 1 hour and visualized with ECL Western Blotting substrate (Pierce) or (for phospho blots) Femto ECL Western blotting substrate (Pierce). Primary antibodies used: phospho-RIPK3 antibody (Genentech), phospho-MLKL antibody (Abcam, ab196436), total RIPK3 (Imgenex, IMG-5523-2), total MLKL (Clone 3H1), total RIPK1 (BD, 610458), total caspase-8 (Enzo, 1G12), actin (Millipore, MAB1501). Secondary antibodies used: anti-rabbit (Jackson ImmunoResearch), anti-mouse (Santa Cruz), anti-rat (Santa Cruz), and anti-goat (Santa Cruz).

### Quantitative RT-PCR

Cells were lysed in RNA Stat 60 (Amsbio). cDNA was synthesized using oligo(dT) and SuperScript III Reverse Transcriptase (Life Tech). Quantitative PCR was performed with SYBR Green (Invitrogen) and a ViiA 7 Real-Time PCR System (Applied Biosystems) using the primers listed below. Three technical replicates were used for each biological sample and CT values were averaged. Average CT values for each measured gene were normalized to average CT values of the housekeeping gene *Gapdh*, and then normalized to a wildtype untreated control sample to obtain ΔΔCT values. Fold change was calculated as 2^(−ΔΔCT) for each sample. Two-three biological replicates were used to generate figures. Primers used: *IP-10* forward 5′-AAGTGCTGCCGTCATTTTCTGCCTC-3′, *IP-10* reverse, 5′-CTTGATGGTCTTAGATTCCGGATTC-3′; *Isg15* forward, 5′-GGTGTCCGTGACTAACTCCAT-3′, *Isg15* reverse, 5′-TGGAAAGGGTAAGACCGTCCT-3′; *Ifit1* forward, 5′-GCCATTCAACTGTCTCCTG-3′, *Ifit1* reverse, 5′-GCTCTGTCTGTGTCATATACC-3′; *Mx1* forward, 5′-GACCATAGGGGTCTTGACCAA-3′, *Mx1* reverse, 5′-AGACTTGCTCTTTCTGAAAAGCC-3′; *Gapdh* forward 5′-GGCAAATTCAACGGCACAGT-3′, *Gapdh* reverse 5′-AGATGGTGATGGGCTTCCC-3′.

## Results

### Introduction of DNA into the cytosol can trigger necroptosis

We sought to understand the cellular response to cytosolic DNA, using primary bone marrow-derived macrophages (BMDM) as an experimental system. We observed that introduction of DNA into the cytosol led to rapid and robust cell death in primary murine BMDM. As has been previously described(28), this cell death response was AIM2- and caspase-1-dependent and morphologically consistent with inflammasome-induced pyroptosis (Fig. 1, A and B). Unexpectedly however, upon addition of the pan-caspase inhibitor zVAD-FMK, macrophages underwent slower but equally robust cell death in

response to DNA transfection (Fig. 1C). This cell death was morphologically consistent with programmed necrosis (Fig. 1B), a lytic cell death program dependent on activation of RIPK3. Indeed, we observed that RIPK3-deficient or MLKL-deficient macrophages were resistant to cell death in response to DNA transfection in combination with zVAD-FMK (Fig. 1C). All tested doses of cytosolic DNA triggered RIPK3-dependent death when combined with zVAD (Fig. S1A). Furthermore, transfection with DNA lead to phosphorylation of RIPK3 and MLKL (Fig. 1D), confirming that DNA stimulation can lead to necroptosis when caspases are suppressed.

Given the robust AIM2 dependent response observed upon introduction of cytosolic DNA alone, we next sought to determine whether components of the AIM2 inflammasome contributed to the cell death we observed upon DNA transfection combined with caspase inhibition. To assess this, we transfected DNA into macrophages lacking the inflammasome component AIM2, and measured their cell death response over time. While pyroptosis could not occur in macrophages missing key inflammasome components, AIM2$^{-/-}$ and Caspase-1/11$^{-/-}$ cells could still undergo necroptosis in response to cytosolic DNA (Fig. 1E) in combination with caspase inhibition. These findings indicate that when AIM2-dependent pyroptosis is prevented, cytosolic DNA can trigger necroptosis via a distinct signaling pathway.

## Cytosolic DNA triggers necroptosis via the cGAS-STING pathway

In an effort to identify the pathway by which cytosolic DNA causes necroptosis, we tested macrophages lacking candidate DNA sensors. A proposed DNA sensor, DAI (encoded by *Zbp1*), has been shown to be important for the induction of necroptosis during herpesvirus infections(2). However, DAI-deficient macrophages were still able to undergo necroptosis following DNA transfection (Fig. 2A), implying that DAI is not required for the induction of necroptosis by a pure DNA ligand. This finding is consistent with recent reports that DAI may sense RNA ligands(29, 30).

The DNA sensor cGAS (encoded by *Mb21d1*) and its signaling adaptor STING (encoded by *Tmem173*) are required for the induction of type-I IFN following detection of DNA in the cytosol. To determine whether activation of the cGAS-STING pathway could also lead to the induction of necroptosis, we transfected DNA into macrophages deficient for either protein. When caspases were suppressed, we found that macrophages lacking cGAS or STING failed to undergo necroptosis after cytosolic DNA stimulation (Fig. 2B), confirming that this pathway is required for the necroptotic response to DNA ligands. cGAS produces a secondary messenger, cyclic GMP-AMP or cGAMP, which binds to and activates STING. We sought to understand whether, like cytosolic DNA, cGAMP could also lead to the induction of necroptosis. Indeed, we observed that upon transfection of cGAMP into macrophages, these cells underwent RIPK3- and MLKL-dependent cell death when caspases were suppressed (Fig. 2C). We observed that like DNA, cGAMP-induced necroptosis required STING, but no longer required cGAS (Fig. 2D). However, unlike DNA, cGAMP treatment in the absence of caspase inhibition did not trigger pyroptosis (Fig. 2, C and D). Additionally, when 100 base pair interferon stimulatory DNA (ISD) was transfected into cells in combination with zVAD treatment, STING- and RIPK3-dependent death was

observed (Fig. S1B), confirming that multiples types of cytosolic DNA can trigger necroptosis. Finally, in order to understand whether DNA ligands could induce necroptosis in additional cell types, primary mouse embryonic fibroblasts (MEFs) were treated with zVAD and transfected with CT DNA or cGAMP. Similar to macrophages, these cells underwent RIPK3-dependent cell death (Fig. S1C). Together, these data indicate that activation of the cGAS-STING pathway can lead to necroptosis in multiple cell types.

## STING-dependent IFN production is necessary but not sufficient to induce necroptosis

The canonical function of the cGAS-STING pathway is the production of type I IFN, and IFN treatment alone has been shown to induce necroptosis under certain conditions(31). We therefore tested whether autocrine or paracrine signaling by IFN produced upon stimulation of the cGAS-STING pathway was necessary for the induction of necroptosis. Following transfection with CT DNA or cGAMP, we observed that IFNαR1-deficient macrophages, which do not respond to IFN, were resistant to necroptosis (Fig. 3, A and B). These results indicate IFN signaling is required to induce necroptosis following cGAS-STING stimulation, echoing results for other RIPK3-activating ligands like TNF, LPS, and poly(I:C) (7). Consistently with this finding, we observed that both STAT1 and STAT2, important signaling molecules downstream of IFN receptor stimulation, were required for cGAMP-induced necroptosis (Fig. S1D). We next tested whether IFN signaling was sufficient to induce necroptosis in macrophages. We found that treatment of WT, but not *Ripk3*$^{-/-}$ primary macrophages with recombinant IFN in combination with zVAD-FMK led to modest necroptotic cell death, and that unlike the robust and consistent necroptotic response observed upon STING activation, the magnitude of cell death triggered by recombinant IFN was highly variable between experiments. (Fig. 3C and fig. S1E). Notably however, the necroptotic response to even supraphysiological doses of recombinant IFNα or IFNβ (Fig. S1F) did not recapitulate that observed upon STING activation. Together, these data indicate that IFN signaling is necessary but not sufficient for the necroptotic response we observe upon activation of the cGAS-STING pathway.

## STING-dependent TNF production is required for induction of necroptosis

Since IFN alone was unable to fully recapitulate the necroptotic response observed upon treatment with DNA or cGAMP, we hypothesized that other STING-dependent signaling might contribute to the activation of the necroptotic cell death program. To identify such a signal, we transfected WT macrophages as well as macrophages lacking STING with cGAMP and assessed cytokine production from these cells by Luminex. We observed that in WT macrophages, but not in *Tmem173*$^{-/-}$ cells, cGAMP treatment led to upregulation of TNF, a cytokine well characterized for its ability to induce programmed necrosis (Fig. 4A). This finding indicated that, as has been shown in other systems(32, 33), STING activation can lead to production of TNF as well as type-I IFN.

We next sought to determine whether STING-dependent production of TNF was required for the cell death response to DNA. To test this, we transfected WT macrophages, as well as cells deficient for TNF, TNFR1 (*Tnfrsf1a)*, or TNFR2 (*Tnfrsf1b)*, with cGAMP. When caspases were suppressed, macrophages deficient in TNF or either of its receptors failed to undergo necroptosis after cGAMP or DNA stimulation (Fig. 4B and fig. S2A),

demonstrating that TNF is essential for robust and efficient necroptosis following activation of the cGAS-STING pathway. As TNFR1 is well characterized as a driver of RIPK1 activation(34), we wanted to test whether the RIPK1 inhibitor, Necrostatin-1, would eliminate DNA- or cGAMP-induced necroptosis. Indeed, addition of Necrostatin-1 significantly reduced necroptosis following treatment with zVAD and either cytosolic DNA or cGAMP (Fig S2C), indicating that TNF-driven RIPK1 activation plays a critical role in DNA-induced necroptosis. While TNFR1 drives RIPK1 activation, we sought to understand the observed requirement for TNFR2 in this setting. One known effect of TNFR2 signaling is the degradation of the cellular inhibitors of apoptosis (cIAPs), which restrict necrosome formation(35), and this de-repression has been reported to be required in combination with RIPK1 activation by TNFR1 to allow necroptosis to proceed(36). To assess this, TNFR1 and TNFR2-deficient cells were treated with zVAD and the IAP antagonist BV6. We observed that cells deficient in TNFR2, but not TNFR1, were sensitized to necroptosis by addition of BV6 (Fig. S2B), consistent with the idea that TNFR2 signaling in this setting acts to de-repress necroptosis by degrading the cIAPs.

As some components of the necroptotic pathway are upregulated in response to IFN or TNF signaling, we sought to ensure that failure to induce necroptosis in TNF or IFNαR1-deficient macrophages was not due to cell intrinsic defect in tonic protein levels. To determine if necroptotic pathway components were present at comparable levels in these cells, WT, *Tnf*$^{-/-}$, and *Ifnar1*$^{-/-}$ macrophages were blotted for RIPK1, Caspase-8, RIPK3, and MLKL. Levels of these proteins were comparable between WT, *Tnf*$^{-/-}$ and *Ifnar1*$^{-/-}$ cells (Fig. 4C), indicating that the resistance of cells lacking TNF or IFN signaling does not arise from a failure to express components of the necroptotic pathway. Given the profound resistance to STING-induced necroptosis observed in both *Tnf*$^{-/-}$ and *Ifnar1*$^{-/-}$ cells, we sought to test whether lack of one of these signaling pathways affected the other. However, we found that upregulation of a panel of IFN-responsive genes by LPS, cGAMP, or recombinant IFN was intact in *Tnf*$^{-/-}$ macrophages (Fig. 4D), indicating that the IFN pathway is intact in these cells. Furthermore, while we saw that cGAMP treatment led to upregulation of TNF message, recombinant IFN treatment failed to upregulate TNF in WT macrophages (Fig. 4E), indicating that IFN signaling alone is not sufficient to initiate TNF signaling. Together, these data indicate that TNF signaling in response to activation of the cGAS-STING pathway is required for necroptosis, and that TNF signaling acts in concert with, but independently from, the IFN pathway to trigger necroptosis in this setting.

## Synergistic IFN and TNF signaling is also required for RIG-I and TLR3-induced necroptosis

Co-activation of both IFN and TNF production is a motif observed downstream of multiple innate immune sensors. Because we observed synergistic signaling of IFN and TNF to trigger necroptosis upon activation of the cGAS-STING pathway, we tested whether similar synergy occurred downstream of other nucleotide sensing pathways. To do this, we assessed the response to 5′-triphosphate RNA, a ligand for the cytosolic RNA sensor RIG-I, and to poly(I:C), a ligand for toll-like receptor 3 (TLR3). Upon transfection of primary macrophages with 5′-triphosphate RNA or poly(I:C) in combination with caspase suppression, we observed robust RIPK3-dependent cell death (Fig. 5A). As expected, necroptosis induced by RIG-I ligand required MAVS, the downstream signaling partner of

RIG-I (Fig. S3A), confirming that this stimulus acted through the RIG-I-MAVS pathway. Analogously, and in accordance with previous studies(7, 37), we observed that poly(I:C) stimulation induced necroptosis in WT but not TLR3- or IFNαR1-deficient macrophages (Fig. S3, B and C). Furthermore, we saw that poly (I:C)-induced necroptosis did not require DAI (*Zbp1*) (Fig. S3D), despite reports of DAI being a putative RNA sensor. When caspases were inhibited, RIG-I ligand similarly required IFNαR1 to induce necroptosis (Fig. 5B), indicating that, like TLR signaling, RIG-I induced necroptosis required an intact IFN pathway.

In order to determine whether these RNA ligands required TNF for efficient necroptosis, we stimulated WT and $Tnf^{-/-}$ macrophages with either 5′ triphosphate or poly(I:C). We found that TNF-deficient macrophages failed to undergo necroptosis following either poly(I:C) or RIG-I ligand stimulation (Fig. 5C), confirming that like DNA, RNA ligands require intact TNF signaling to induce necroptosis. Consistent with this, we saw that phosphorylation of RIPK3 was absent following poly(I:C) treatment in $Ifnar^{-/-}$ macrophages, and significantly reduced in $Tnf^{-/-}$ cells (Fig. 5D), indicating a requirement for both TNF and IFN signaling downstream of poly(I:C) stimulation.

Finally, we sought to determine whether the moderate levels of cell death seen in WT macrophages following high dose IFN treatment were also dependent on the presence of TNF. To test this, we treated WT and TNF-deficient macrophages with a high dose of IFN and inhibited caspases. We found that $Tnf^{-/-}$ macrophages were completely resistant to IFN-induced necroptosis (Fig. 5E), indicating that even necroptosis induced by direct IFN stimulation requires TNF production and signaling. Taken together, these data indicate a broad requirement for synergy between IFN and TNF signaling for the induction of necroptosis downstream of multiple innate immune sensing pathways.

## STING agonists induce sterile shock in mice

It has previously been established that activation of RIPK1 and RIPK3 contributes to the mortality associated with sterile shock models following administration of high doses of TNF(38). Because we observed a requirement for STING-dependent TNF production for the induction of necroptosis *in vitro*, we wondered whether systemic STING activation *in vivo* might also lead to RIPK3-dependent pathology. Notably, STING agonists are currently in clinical development as tumor immunotherapy agents, but potential adverse responses to systemic administration of these agents have not been studied. DMXAA is a potent activator of murine STING that has been shown to have anti-tumor properties in mouse models(39, 40). Notably, the action of DMXAA is associated with production of TNF and other inflammatory cytokines(41) and therefore provided an ideal tool to test if STING activation could induce RIPK3 activation *in vivo*. Consistent with its role as a STING agonist, we found that DMXAA, in combination with zVAD, induced robust necroptosis in primary macrophages *in vitro* in a STING and RIPK3-dependent manner (Fig. S4A), analogous to the effects of cGAMP. To assess the systemic response to STING activation, we administered DMXAA intraperitoneally and monitored mice for clinical signs of shock, such as hypothermia, lethargy, ocular secretions, and the production of pro-inflammatory cytokines. We found that DMXAA induced significant mortality in C57BL/6J (B6/J WT)

animals, while STING-deficient animals were completely resistant to mortality (Fig. 6A). Even more strikingly, STING-deficient mice were protected from all observable signs of shock, and serum collected from these mice lacked detectible levels of the pro-inflammatory cytokine interleukin-6 (IL-6) and TNFα (Fig. 6A and fig. S4, B–D). These findings demonstrate that systemic DMXAA administration causes shock-like symptoms, and that this response is wholly dependent on STING signaling.

### Systemic shock induced by STING activation engages TNF, IFN, and necroptotic signaling

We next sought to test whether the sterile shock and mortality triggered by systemic STING activation *in vivo* involved engagement of TNF and/or IFN signaling. To do this, we administered DMXAA to *Tnf*$^{-/-}$ and *Ifnar1*$^{-/-}$ animals. Whereas a majority of WT animals succumbed to disease within 24 hours, both *Tnf*$^{-/-}$ and *Ifnar1*$^{-/-}$ animals were completely resistant to mortality following DMXAA injection (Fig. 6B). Furthermore, mice lacking TNF or IFNAR1 showed a reduction in the inflammatory marker IL-6 upon systemic STING activation, though this reached statistical significance only in the case of TNF knockout (Fig. 6B and fig. S4D).

Given the synergy observed between IFN and TNF signaling *in vitro*, together with our finding that both pathways are involved in STING-driven shock *in vivo*, we next tested whether engagement of necroptotic signaling plays a role in the pathology observed upon DMXAA administration. To do this, we administered DMXAA to animals lacking either MLKL or RIPK3. *Mlkl*$^{-/-}$ animals were also significantly rescued from the lethal effects of STING activation, though not completely resistant (Fig. 6C). *Ripk3*$^{-/-}$ mice are backcrossed to the C57BL/6N strain background, while other mice used in this study are congenic with the C57BL/6J background. Because of reported differences between these sub-strains in other models of sterile shock(42), we compared *Ripk3*$^{-/-}$ mice to littermate-matched WT or heterozygous animals. Both RIPK3-deficient and heterozygous animals were significantly rescued from mortality, while DMXAA was uniformly lethal to their wild-type littermates (Fig. 6D). Interestingly, whereas C57BL/6J mice have been shown to be more susceptible to recombinant TNF injection than C57BL/6N mice(42), we found the opposite following DMXAA administration (Fig. 6A–D). Notably, we found that serum from mice lacking RIPK3 or MLKL had levels of the pro-inflammatory cytokine IL-6 comparable to those observed in WT mice following DMXAA treatment (Fig. 6C and D), suggesting that while the pathological response to inflammatory signaling is attenuated in these mice, the inflammatory signals themselves remain. Together, our findings indicate that activation of the cGAS-STING pathway *in vivo* causes activation of both IFN and TNF signaling, and that synergy between these pathways engages RIPK3 and MLKL to cause lethal shock.

## Discussion

The sensing of foreign nucleic acids within the cell is a key initiator of the immune response to invading pathogens, and it can trigger diverse outcomes including both transcriptional changes and cell death. We show that following DNA detection, the cGAS-STING pathway can trigger necroptosis in primary macrophages when caspases are suppressed. Notably, this cell death response requires STING-dependent production of both type-I interferon and

TNF, and the induction of necroptosis by STING activation involves reciprocal, synergistic signaling by these two pathways. While a similar finding of STING-dependent death was noted in a recent study using infection of L929 cells(17), our study provides a more complete understanding of this phenomenon through the use of primary cells and purified ligands, and avoids the confounding fact that L929 cells constitutively produce and respond to TNF in an autocrine manner(18). In addition, as the type I IFN and TNF signaling pathways are both activated downstream of other ligands, we show that RNA detection though both the RIG-I-MAVS pathway and the TLR3 pathway can trigger RIPK3 activation via a similar mechanism when caspases are suppressed, again requiring synergistic signaling through IFN and TNF.

The cGAS-STING pathway has been shown to play a critical role in the response to numerous DNA virus infections, through the production of type I IFN and resulting antiviral state(8). Viruses such as vaccinia trigger STING activation(14) but also encode caspase inhibitors that have been shown to inhibit caspase-8 and lead to RIPK3 activation(43). While STING-dependent IFN production by infected cells may lead to the induction of an antiviral state in neighboring cells by paracrine signaling, our data would suggest that it may also act in an autocrine manner to induce death of the infected cell itself, thereby eliminating the replicative niche of the virus. This implies that RIPK3 activation represents an arm of the IFN-driven antiviral response, triggered only when the cell is exposed to coincident IFN and TNF signaling, as well as viral caspase suppression. This requirement may allow for communication of the need for an antiviral response through paracrine signaling, and concurrent elimination of the infected cells themselves.

In addition to its antiviral role, recent work has established STING as a mediator of beneficial anti-tumor immune responses(44). DMXAA was a clinical failure, because it activates only murine, but not human, STING(45). However, stabilized cyclic dinucleotide compounds that activate human STING are currently in clinical trials as tumor immunotherapy agents. These compounds require STING for their efficacy, and lead to the production of both TNF and IFN(40). Our data indicate that dose-limiting toxicity of these agents likely involves engagement of the necroptotic pathway. While the long-term efficacy and toxicity of these compounds at clinically relevant doses has not yet been established, our findings indicate that modulation of the necroptotic pathway may help to alleviate any shock-like adverse reactions to these drugs. Conversely, it is unknown whether the antitumor effects of cyclic dinucleotides involve activation of RIPK3 downstream of STING signaling within the tumor microenvironment. It is possible that RIPK3 engagement and necroptosis contributes to the efficacy of STING agonists, as antigens derived from necroptotic cells activate T cell responses more readily than those derived from apoptotic cells and might better inform a cellular immune response to tumors(46).

A surprising facet of our data is the finding that both TNF and IFN signaling are required for induction of necroptosis by stimulation of TLR3, a pathway in which the RHIM-containing adapter TRIF is able to directly engage the RIP kinases(37, 47). This requirement is not explained by TNF or IFN-mediated induction of known components of this signaling pathway. Furthermore, we show that necroptosis triggered by IFN signaling in the absence of pathogen-associated ligands requires TNF signaling, despite a lack of TNF induction

upon IFN treatment. Thus, at least in this setting, it appears that tonic levels of TNF signaling are required to maintain cells in a necroptosis-competent state. This state likely reflects a combination of RIPK1 activation via TNFR1, and control of cIAP levels via TNFR2. How TNF and IFN interface in this setting remains to be understood. Future work will assess the role of these two pathways in the induction of necroptosis in infection and co-infection models where both IFN and TNF signaling is critical for pathogen clearance.

## Supplementary Material

Refer to Web version on PubMed Central for supplementary material.

## Acknowledgments

This work is supported by NIH grants 1R01AI108685 and 1R21NS101542 (to AO), 1R01AI084914 (to DS), 1ZIAES10328601 (to JM) and T32GM007270 (to MB).

The authors thank Dr. Joshua Woodward for provision of reagents, and Drs. William Kaiser, Michael Gale, and Herbert W. Virgin for assistance in procuring mouse strains.

## References

1. Linkermann A, Green DR. Necroptosis. N Engl J Med. 2014; 370:455–465. [PubMed: 24476434]
2. Upton JW, Kaiser WJ, Mocarski ES. DAI/ZBP1/DLM-1 complexes with RIP3 to mediate virus-induced programmed necrosis that is targeted by murine cytomegalovirus vIRA. Cell Host and Microbe. 2012; 11:290–297. [PubMed: 22423968]
3. Upton JW, Kaiser WJ, Mocarski ES. Virus Inhibition of RIP3-Dependent Necrosis. Cell Host and Microbe. 2010; 7:302–313. [PubMed: 20413098]
4. Nogusa S, Thapa RJ, Dillon CP, Liedmann S, Oguin TH, Ingram JP, Rodriguez DA, Kosoff R, Sharma S, Sturm O, Verbist K, Gough PJ, Bertin J, Hartmann BM, Sealfon SC, Kaiser WJ, Mocarski ES, López CB, Thomas PG, Oberst A, Green DR, Balachandran S. RIPK3 Activates Parallel Pathways of MLKL-Driven Necroptosis and FADD-Mediated Apoptosis to Protect against Influenza A Virus. Cell Host and Microbe. 2016; 20:13–24. [PubMed: 27321907]
5. Huang Z, Wu SQ, Liang Y, Zhou X, Chen W, Li L, Wu J, Zhuang Q, Chen C, Li J, Zhong CQ, Xia W, Zhou R, Zheng C, Han J. RIP1/RIP3 binding to HSV-1 ICP6 initiates necroptosis to restrict virus propagation in mice. Cell Host and Microbe. 2015; 17:229–242. [PubMed: 25674982]
6. Daniels BP, Snyder AG, Olsen TM, Orozco S, Oguin TH, Tait SWG, Martinez J, Gale M, Loo YM, Oberst A. RIPK3 Restricts Viral Pathogenesis via Cell Death-Independent Neuroinflammation. Cell. 2017; 169:301–313.e11. [PubMed: 28366204]
7. McComb S, Cessford E, Alturki NA, Joseph J, Shutinoski B, Startek JB, Gamero AM, Mossman KL, Sad S. Type-I interferon signaling through ISGF3 complex is required for sustained Rip3 activation and necroptosis in macrophages. Proceedings of the National Academy of Sciences. 2014; 111:E3206–13.
8. Chen Q, Sun L, Chen ZJ. Regulation and function of the cGAS–STING pathway of cytosolic DNA sensing. Nature Immunology. 2016; 17:1142–1149. [PubMed: 27648547]
9. Sun L, Sun L, Wu J, Wu J, Du F, Du F, Chen X, Chen X, Chen ZJ, Chen ZJ. Cyclic GMP-AMP Synthase Is a Cytosolic DNA Sensor That Activates the Type I Interferon Pathway. Science. 2013; 339:786–791. [PubMed: 23258413]
10. Zhang X, Shi H, Wu J, Zhang X, Sun L, Chen C, Chen ZJ. Cyclic GMP-AMP Containing Mixed Phosphodiester Linkages Is An Endogenous High-Affinity Ligand for STING. Mol Cell. 2013; 51:226–235. [PubMed: 23747010]
11. Stetson DB, Medzhitov R. Recognition of Cytosolic DNA Activates an IRF3-Dependent Innate Immune Response. Immunity. 2006; 24:93–103. [PubMed: 16413926]

12. Reinert LS, Lopušná K, Winther H, Sun C, Thomsen MK, Nandakumar R, Mogensen TH, Meyer M, Vægter C, Nyengaard JR, Fitzgerald KA, Paludan SR. Sensing of HSV-1 by the cGAS-STING pathway in microglia orchestrates antiviral defence in the CNS. Nat Comms. 2016; 7:13348.
13. Ishikawa H, Ma Z, Barber GN. STING regulates intracellular DNA-mediated, type I interferon-dependent innate immunity. Nature. 2009; 461:788–792. [PubMed: 19776740]
14. Schoggins JW, MacDuff DA, Imanaka N, Gainey MD, Shrestha B, Eitson JL, Mar KB, Richardson RB, Ratushny AV, Litvak V, Dabelic R, Manicassamy B, Aitchison JD, Aderem A, Elliott RM, García-Sastre A, Racaniello V, Snijder EJ, Yokoyama WM, Diamond MS, Virgin HW, Rice CM. Pan-viral specificity of IFN-induced genes reveals new roles for cGAS in innate immunity. Nature. 2015; 505:691–695.
15. Barber GN. STING: infection, inflammation and cancer. Nature Publishing Group. 2015; 15:760–770.
16. Cho YS, Challa S, Moquin D, Genga R, Ray TD, Guildford M. Phosphorylation-driven assembly of the RIP1-RIP3 complex regulates programmed necrosis and virus-induced inflammation. Cell. 2009; 137:1112–1123. [PubMed: 19524513]
17. Schock SN, Chandra NV, Sun Y, Irie T, Kitagawa Y, Gotoh Bin, Gotoh B, Coscoy L, Winoto A. Induction of necroptotic cell death by viral activation of the RIG-I or STING pathway. Cell Death Differ. 2017; 24:615–625. [PubMed: 28060376]
18. Wu YT, Tan HL, Huang Q, Sun XJ, Zhu X, Shen HM. zVAD-induced necroptosis in L929 cells depends on autocrine production of TNFα mediated by the PKC-MAPKs-AP-1 pathway. Cell Death Differ. 2011; 18:26–37. [PubMed: 20539307]
19. Saito T, Owen DM, Jiang F, Marcotrigiano J, Gale M. Innate immunity induced by composition-dependent RIG-I recognition of hepatitis C virus RNA. Nature. 2008; 454:523–527. [PubMed: 18548002]
20. Gray EE, Treuting PM, Woodward JJ, Stetson DB. Cutting Edge: cGAS Is Required for Lethal Autoimmune Disease in the Trex1-Deficient Mouse Model of Aicardi-Goutières Syndrome. J Immunol. 2015; 195:1939–1943. [PubMed: 26223655]
21. Gall A, Treuting P, Elkon KB, Loo YM, Gale M, Barber GN, Stetson DB. Autoimmunity initiates in nonhematopoietic cells and progresses via lymphocytes in an interferon-dependent autoimmune disease. Immunity. 2012; 36:120–131. [PubMed: 22284419]
22. Brunette RL, Young JM, Whitley DG, Brodsky IE, Malik HS, Stetson DB. Extensive evolutionary and functional diversity among mammalian AIM2-like receptors. Journal of Experimental Medicine. 2012; 209:1969–1983. [PubMed: 23045604]
23. Ishii KJ, Kawagoe T, Koyama S, Matsui K, Kumar H, Kawai T, Uematsu S, Takeuchi O, Takeshita F, Coban C, Akira S. TANK-binding kinase-1 delineates innate and adaptive immune responses to DNA vaccines. Nature. 2008; 451:725–729. [PubMed: 18256672]
24. Kuida K, Lippke JA, Ku G, Harding MW, Livingston DJ, Su MS, Flavell RA. Altered cytokine export and apoptosis in mice deficient in interleukin-1 beta converting enzyme. Science. 1995; 267:2000–2003. [PubMed: 7535475]
25. Newton K, Sun X, Dixit VM. Kinase RIP3 is dispensable for normal NF-κBs, signaling by the B-cell and T-cell receptors, tumor necrosis factor receptor 1, and Toll-like receptors 2 and 4. Molecular and Cellular Biology. 2004
26. Murphy JM, Czabotar PE, Hildebrand JM, Lucet IS, Zhang JG, Alvarez-Diaz S, Lewis R, Lalaoui N, Metcalf D, Webb AI, Young SN, Varghese LN, Tannahill GM, Hatchell EC, Majewski IJ, Okamoto T, Dobson RCJ, Hilton DJ, Babon JJ, Nicola NA, Strasser A, Silke J, Alexander WS. The pseudokinase MLKL mediates necroptosis via a molecular switch mechanism. Immunity. 2013; 39:443–453. [PubMed: 24012422]
27. Alexopoulou L, Holt AC, Medzhitov R, Flavell RA. Recognition of double-stranded RNA and activation of NF-kappaB by Toll-like receptor 3. Nature. 2001; 413:732–738. [PubMed: 11607032]
28. Hornung V, Ablasser A, Charrel-Dennis M, Bauernfeind F, Horvath G, Caffrey DR, Latz E, Fitzgerald KA. AIM2 recognizes cytosolic dsDNA and forms a caspase-1-activating inflammasome with ASC. Nature. 2009; 458:514–518. [PubMed: 19158675]

29. Maelfait J, Liverpool L, Bridgeman A, Ragan KB, Upton JW, Rehwinkel J. Sensing of viral and endogenous RNA by ZBP1/DAI induces necroptosis. The EMBO Journal. 2017:e201796476.

30. Thapa RJ, Ingram JP, Ragan KB, Nogusa S, Boyd DF, Benitez AA, Sridharan H, Kosoff R, Shubina M, Landsteiner VJ, Andrake M, Vogel P, Sigal LJ, tenOever BR, Thomas PG, Upton JW, Balachandran S. DAI Senses Influenza A Virus Genomic RNA and Activates RIPK3-Dependent Cell Death. Cell Host and Microbe. 2016; 20:674–681. [PubMed: 27746097]

31. Thapa RJ, Nogusa S, Rall GF, Balachandran S. Interferon-induced RIP1/RIP3-mediated necrosis requires PKR and is licensed by FADD and caspases. Proceedings of the National Academy of Sciences. 2013; 110:E3109–18.

32. Blaauboer SM, Blaauboer SM, Gabrielle VD, Gabrielle VD, Jin L, Jin L. MPYS/STING-Mediated TNF-, Not Type I IFN, Is Essential for the Mucosal Adjuvant Activity of (3′-5′)-Cyclic-Di-Guanosine-Monophosphate In Vivo. The Journal of Immunology. 2013; 192:492–502. [PubMed: 24307739]

33. Ahn J, Gutman D, Saijo S, Barber GN. STING manifests self DNA-dependent inflammatory disease. Proceedings of the National Academy of Sciences. 2012; 109:19386–19391.

34. Kelliher MA, Grimm S, Ishida Y, Kuo F, Stanger BZ, Leder P. The death domain kinase RIP mediates the TNF-induced NF-kappaB signal. Immunity. 1998; 8:297–303. [PubMed: 9529147]

35. Feoktistova M, Geserick P, Kellert B, Dimitrova DP, Langlais C, Hupe M, Cain K, MacFarlane M, Häcker G, Leverkus M. cIAPs block Ripoptosome formation, a RIP1/caspase-8 containing intracellular cell death complex differentially regulated by cFLIP isoforms. Mol Cell. 2011; 43:449–463. [PubMed: 21737330]

36. Siegmund D, Kums J, Ehrenschwender M, Wajant H. Activation of TNFR2 sensitizes macrophages for TNFR1-mediated necroptosis. Cell Death Dis. 2016; 7:e2375. [PubMed: 27899821]

37. He S, Liang Y, Shao F, Wang X. Toll-like receptors activate programmed necrosis in macrophages through a receptor-interacting kinase-3-mediated pathway. Proceedings of the National Academy of Sciences. 2011; 108:20054–20059.

38. Duprez L, Takahashi N, Van Hauwermeiren F, Vandendriessche B, Goossens V, Vanden Berghe T, Declercq W, Libert C, Cauwels A, Vandenabeele P. RIP kinase-dependent necrosis drives lethal systemic inflammatory response syndrome. Immunity. 2011; 35:908–918. [PubMed: 22195746]

39. Baguley BC, Ching LM. Immunomodulatory actions of xanthenone anticancer agents. BioDrugs. 1997; 8:119–127. [PubMed: 18020500]

40. Corrales L, Glickman LH, McWhirter SM, Kanne DB, Sivick KE, Katibah GE, Woo SR, Lemmens E, Banda T, Leong JJ, Metchette K, Dubensky TW, Gajewski TF. Direct Activation of STING in the Tumor Microenvironment Leads to Potent and Systemic Tumor Regression and Immunity. Cell Rep. 2015; 11:1018–1030. [PubMed: 25959818]

41. Perera PY, Barber SA, Ching LM, Vogel SN. Activation of LPS-inducible genes by the antitumor agent 5,6-dimethylxanthenone-4-acetic acid in primary murine macrophages. Dissection of signaling pathways leading to gene induction and tyrosine phosphorylation. The Journal of Immunology. 1994; 153:4684–4693. [PubMed: 7525711]

42. Vanden Berghe T, Hulpiau P, Martens L, Vandenbroucke RE, Van Wonterghem E, Perry SW, Bruggeman I, Divert T, Choi SM, Vuylsteke M, Shestopalov VI, Libert C, Vandenabeele P. Passenger Mutations Confound Interpretation of All Genetically Modified Congenic Mice. Immunity. 2015; 43:200–209. [PubMed: 26163370]

43. Li M, Beg AA. Induction of Necrotic-Like Cell Death by Tumor Necrosis Factor Alpha and Caspase Inhibitors: Novel Mechanism for Killing Virus-Infected Cells. Journal of virology. 2000; 74:7470–7477. [PubMed: 10906200]

44. Woo SR, Fuertes MB, Corrales L, Spranger S, Furdyna MJ, Leung MYK, Duggan R, Wang Y, Barber GN, Fitzgerald KA, Alegre ML, Gajewski TF. STING-dependent cytosolic DNA sensing mediates innate immune recognition of immunogenic tumors. Immunity. 2014; 41:830–842. [PubMed: 25517615]

45. Conlon J, Conlon J, Burdette DL, Burdette DL, Sharma S, Sharma S, Bhat N, Bhat N, Thompson M, Thompson M, Jiang Z, Jiang Z, Rathinam VAK, Rathinam VAK, Monks B, Monks B, Jin T, Jin T, Xiao TS, Xiao TS, Vogel SN, Vogel SN, Vance RE, Vance RE, Fitzgerald KA, Fitzgerald KA. Mouse, but not Human STING, Binds and Signals in Response to the Vascular Disrupting Agent

5,6-Dimethylxanthenone-4-Acetic Acid. The Journal of Immunology. 2013; 190:5216–5225. [PubMed: 23585680]

46. Yatim N, Jusforgues-Saklani H, Orozco S, Schulz O, Barreira da Silva R, Reis e Sousa C, Green DR, Oberst A, Albert ML. RIPK1 and NF-κB signaling in dying cells determines cross-priming of $CD8^+$ T cells. Science. 2015; 350:328–334. [PubMed: 26405229]
47. Kaiser WJ, Sridharan H, Huang C, Mandal P, Upton JW, Gough PJ, Sehon CA, Marquis RW, Bertin J, Mocarski ES. Toll-like receptor 3-mediated necrosis via TRIF, RIP3, and MLKL. J Biol Chem. 2013; 288:31268–31279. [PubMed: 24019532]

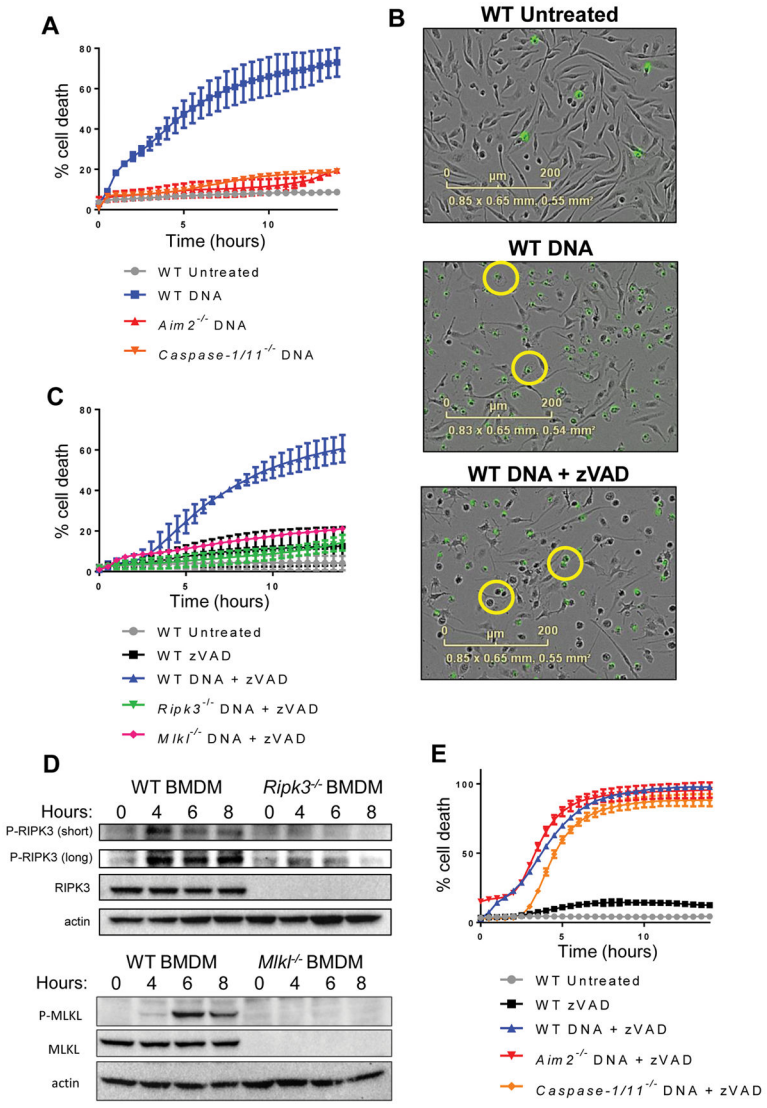


**Figure 1. Introduction of DNA into the cytosol can trigger necroptotic cell death**

(A) Kinetic cell death of WT, *Aim2*$^{-/-}$, or *Caspase-1/11*$^{-/-}$ primary bone marrow-derived macrophages (BMDM) after transfection with 2 μg/ml DNA. Death measured by uptake of cell impermeable Sytox green dye, and normalized to starting number of cells stained with cell permeable Syto green dye to calculate percent cell death. Error bars represent SD from three independent experiments. (B) IncuCyte images of WT BMDM treated with 2 μg/ml DNA, or 2 μg/ml DNA + 50 μM zVAD. Sytox Green staining is shown in green. (C) Kinetic cell death of WT, *Ripk3*$^{-/-}$, or *Mlkl*$^{-/-}$ BMDM after treatment with 2 μg/ml cytosolic DNA and 50 uM pan-caspase inhibitor zVAD. (D) Western blot analysis of phosphorylated RIPK3 or MLKL at short and long exposure following treatment of 5 μg/ml cytosolic DNA and 50 μM pan-caspase inhibitor zVAD in WT, *Ripk3*$^{-/-}$, or *Mlkl*$^{-/-}$ BMDM. “z” in hours indicates zVAD alone control. (E) Kinetic cell death of WT, *Aim2*$^{-/-}$, or *Casp1/11*$^{-/-}$ BMDM after treatment with 2 μg/ml cytosolic DNA and 50 μM pan-caspase inhibitor zVAD.

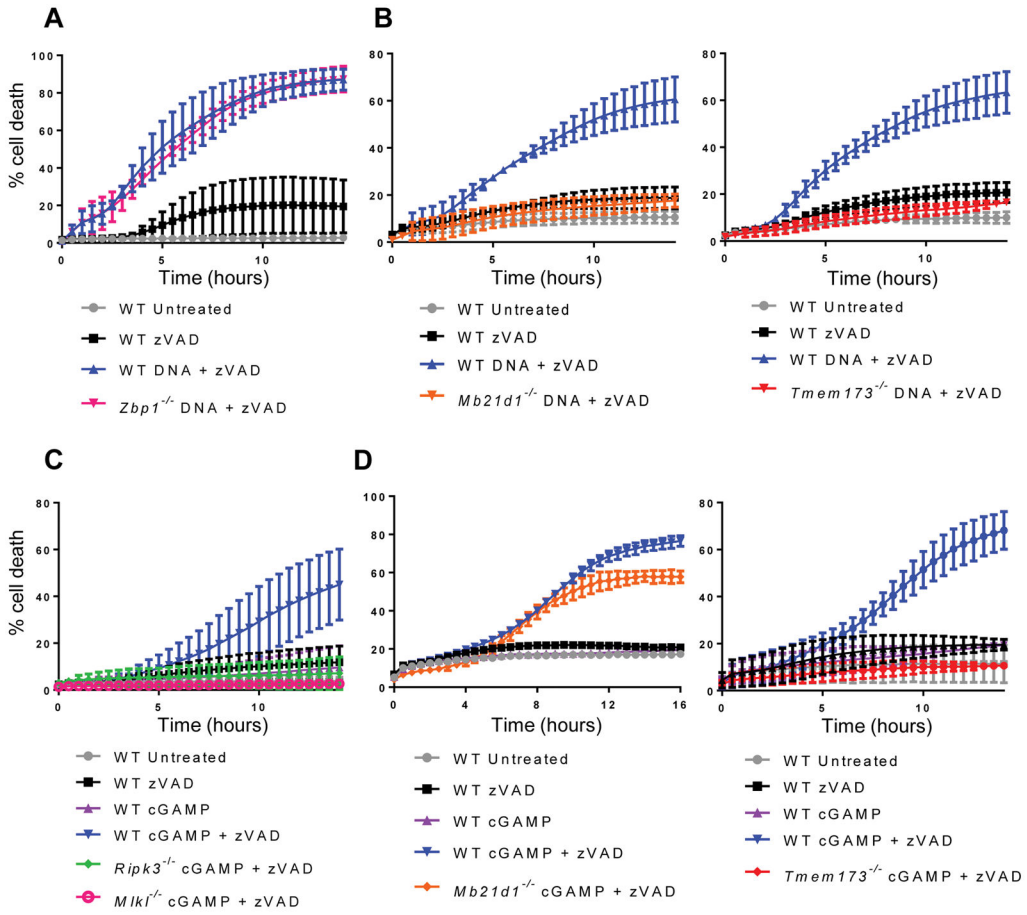


**Figure 2. Cytosolic DNA triggers necroptosis via the cGAS-STING pathway**

(A) Kinetic cell death of WT or *Zbp1*$^{-/-}$ BMDM after treatment with 2 μg/ml cytosolic DNA and 50 μM pan-caspase inhibitor zVAD. (B) Kinetic cell death of WT, *Mb21d1*$^{-/-}$, *Tmem173*$^{-/-}$ BMDM after treatment with 2 μg/ml cytosolic DNA and 50 μM pan-caspase inhibitor zVAD. (C) Kinetic cell death of WT, *Ripk3*$^{-/-}$, or *Mlkl*$^{-/-}$ BMDM after treatment with 2 μg/ml cGAMP and 25 μM pan-caspase inhibitor zVAD. (D) Kinetic cell death of WT, *Mb21d1*$^{-/-}$, or *Tmem173*$^{-/-}$ BMDM after treatment with 2 μg/ml cGAMP and 25 μM pan-caspase inhibitor zVAD.

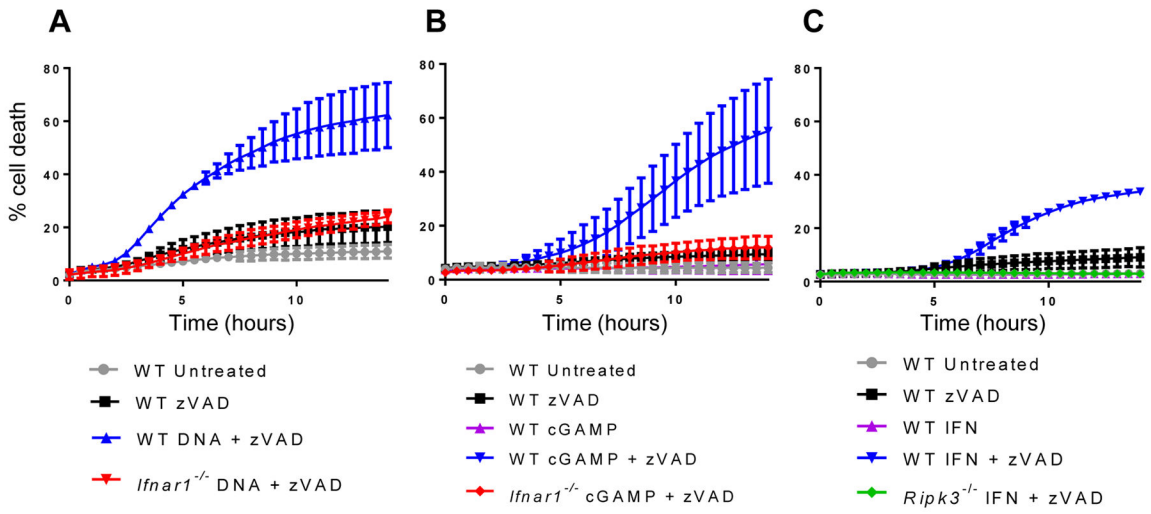


**Figure 3. STING-dependent IFN production is necessary but not sufficient to induce necroptosis**

(A) Kinetic cell death of WT or *Ifnar1*$^{-/-}$ BMDM after treatment with 2 μg/ml cytosolic DNA and 50 μM pan-caspase inhibitor zVAD. (B) Kinetic cell death of WT or *Ifnar1*$^{-/-}$ BMDM after treatment with 2 μg/ml cGAMP and 25 μM pan-caspase inhibitor zVAD. (C) Kinetic cell death of WT or *Ripk3*$^{-/-}$ BMDM after treatment with 100 units/ml recombinant IFN and 25 μM pan-caspase inhibitor zVAD.

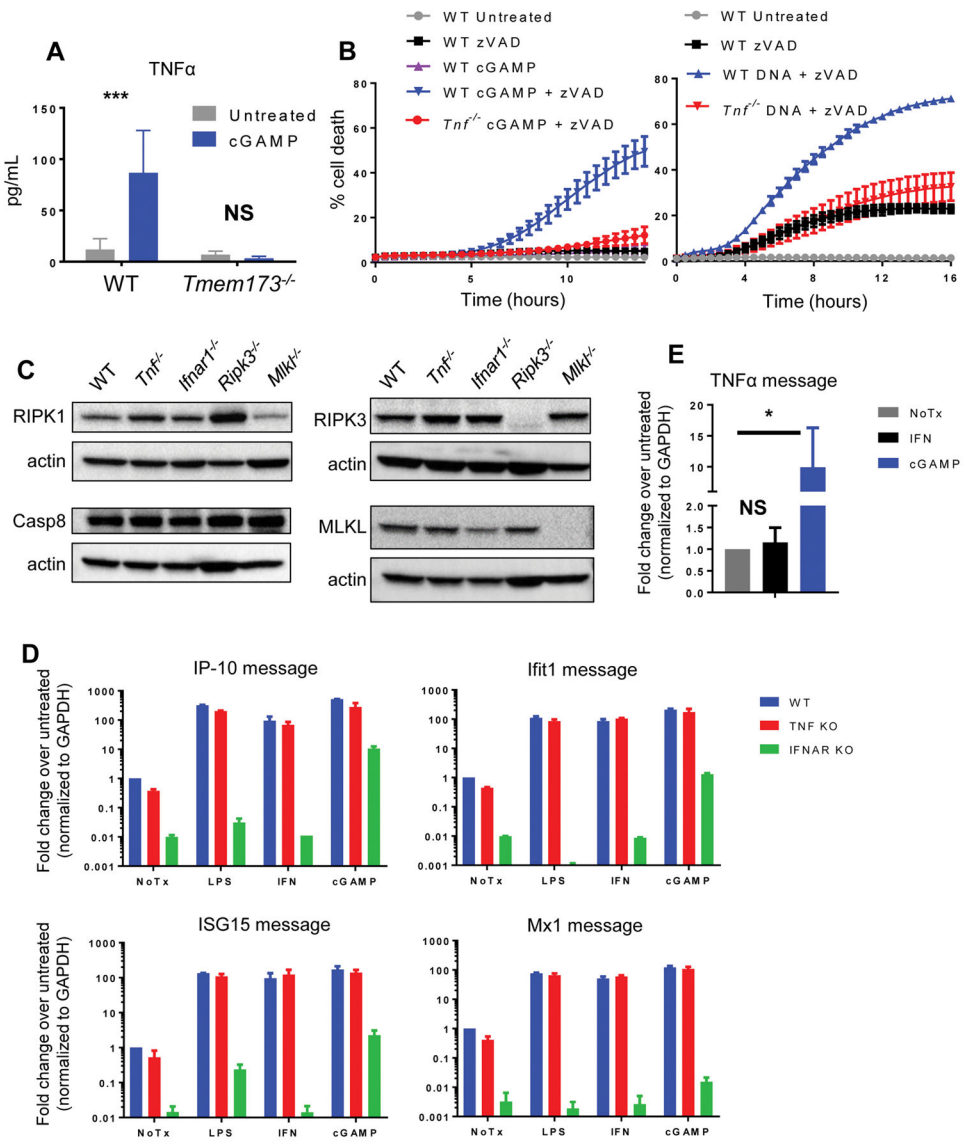


**Figure 4. STING-dependent TNF production is required for the induction of necroptosis**

Luminex analysis of TNFα protein levels in supernatants from WT or *Tmem173*$^{-/-}$ BMDM following treatment with 5 μg/ml cGAMP. Error bars represent SD for three independent experiments. (B) Kinetic cell death of WT or *Tnf*$^{-/-}$ BMDM after treatment with 2 μg/ml cGAMP and 25 μM pan-caspase inhibitor zVAD, or 1 μg/ml cytosolic DNA and 50 μM pan-caspase inhibitor zVAD. (C) Western blot analysis of RIPK1, Caspase-8, RIPK3, and MLKL protein levels at steady state in WT, *Tnf*$^{-/-}$, *Ifnar1*$^{-/-}$, *Ripk3*$^{-/-}$, or *Mlkl*$^{-/-}$ BMDM. (D) Quantitative PCR analysis of interferon stimulated genes (IP-10, Ifit1, ISG15, Mx1) in WT, *Tnf*$^{-/-}$, or *Ifnar1*$^{-/-}$ BMDM following 6 hour treatment with 200 ng/ml LPS, 100 units/ml recombinant IFN, or 5 μg/ml cGAMP. Error bars represent SD for two independent experiments with three technical replicates. Raw values were normalized to housekeeping gene *Gapdh* and then to the WT untreated sample. (E) Quantitative PCR analysis of *Tnf* in WT BMDM following 6 hour treatment with 100 units/ml recombinant IFN or 5 μg/ml cGAMP. *p < 0.05, **p < 0.01, ***p < 0.001

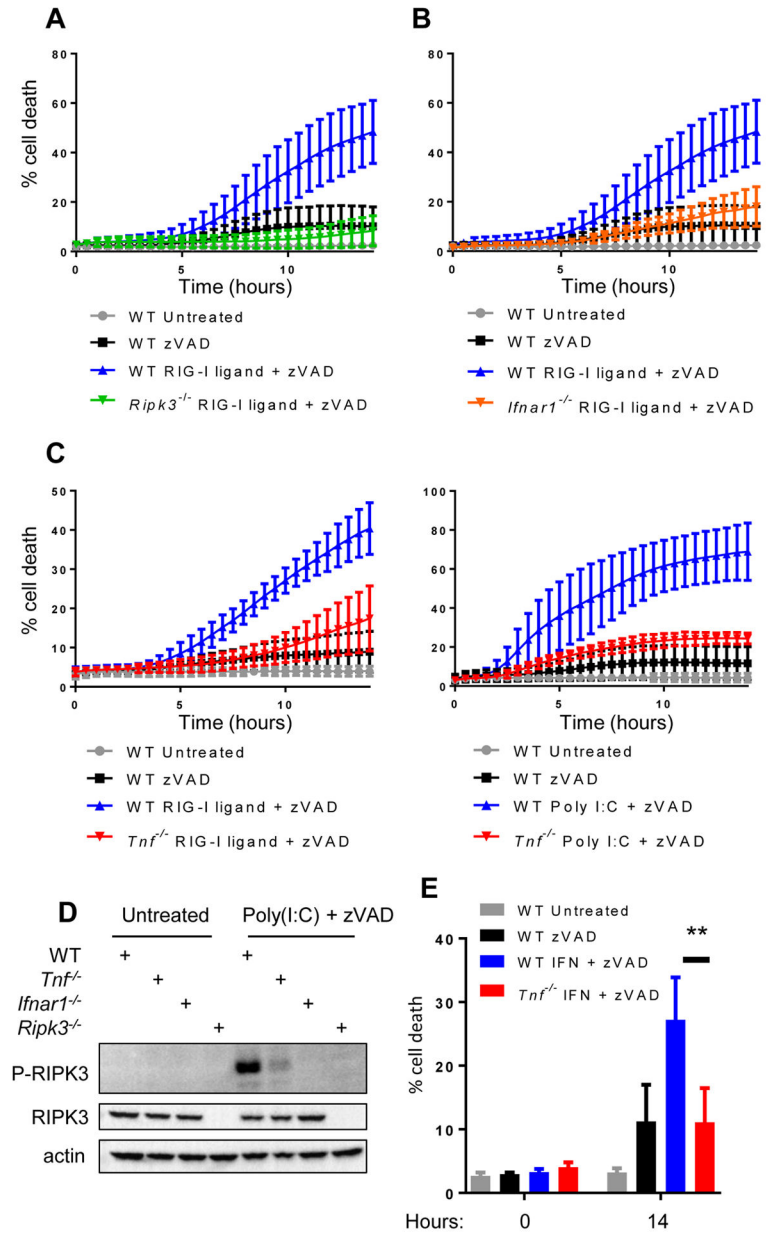


**Figure 5. Synergistic TNF and IFN singaling is required for necroptosis downstream of TLR3 and RIG-I**

(A) Kinetic cell death of WT or *Ripk3*$^{-/-}$ BMDM after treatment with 1 μg/ml 5′-tri-phosphate RNA (RIG-I ligand) and 25 μM pan-caspase inhibitor zVAD. (B) Kinetic cell death of WT or *Ifnar1*$^{-/-}$ BMDM after treatment with 1 μg/ml tri-phosphate RNA (RIG-I ligand) and 25 μM pan-caspase inhibitor zVAD. (C) Kinetic cell death of WT or *Tnf*$^{-/-}$ BMDM after treatment with 1 μg/ml tri-phosphate RNA (RIG-I ligand) and 25 μM pan-caspase inhibitor zVAD or 1 μg/ml poly(I:C) and 25 μM pan-caspase inhibitor zVAD. (D) Western blot analysis of phosphorylated RIPK3 in WT, *Tnf*$^{-/-}$, *Ifnar1*$^{-/-}$, or *Ripk3*$^{-/-}$BMDM following treatment with 2 μg/ml poly(I:C). Cells were harvested 8 hours

post treatment. (E) Cell death analysis of WT or *Tnf*$^{-/-}$ BMDM after treatment with 100 units/ml recombinant IFN and 25 μM pan-caspase inhibitor zVAD.

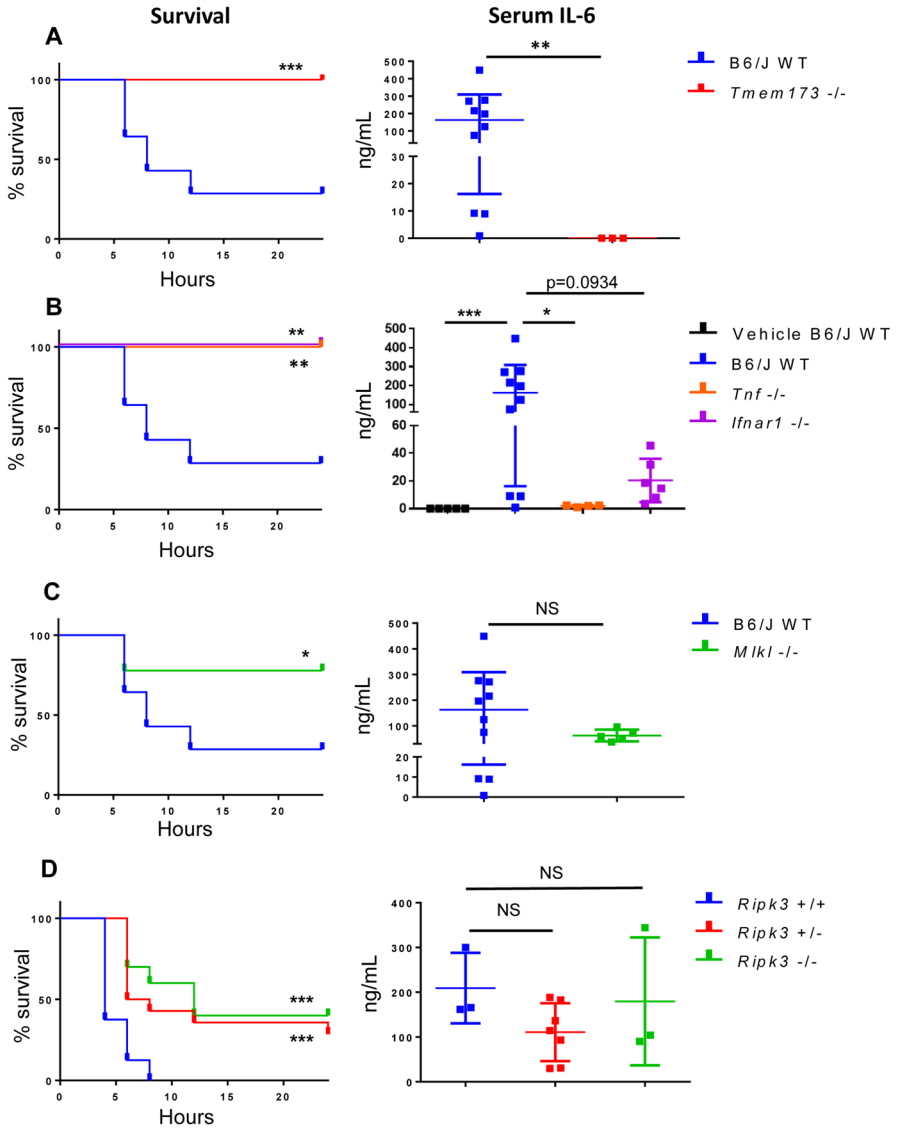


**Figure 6. STING agonists induce sterile shock that engages TNF, IFN, and necroptosis *in vivo***

(A) Survival analysis and serum IL-6 of age/sex matched WT C57BL/6J and *Tmem173*$^{-/-}$ mice after intraperitoneal injection of 40 mg/kg DMXAA. Serum was collected 6 hours post treatment. (B) Survival analysis and serum IL-6 of age/sex matched WT C57BL/6J, *Tnf*$^{-/-}$, and *Ifnar1*$^{-/-}$ mice after intraperitoneal injection of 40 mg/kg DMXAA. (C) Survival analysis and serum IL-6 of age/sex matched WT C57BL/6J and *Mlkl*$^{-/-}$ mice after intraperitoneal injection of 40 mg/kg DMXAA. (D) Survival analysis and serum IL-6 of littermate C57BL/6N *Ripk3*$^{+/+}$, *Ripk3*$^{+/-}$, *Ripk3*$^{-/-}$ mice after intraperitoneal injection of 40 mg/kg DMXAA. *p < 0.05, **p < 0.01, ***p < 0.001. All data is pooled from three or more independent experiments. B6/J WT data is pooled from all experiments and separated to different panels for ease of data comparison within panel.